Chapter 3
Detecting Inequalities from Earth Observation–Derived Global Societal Variables

Daniele Ehrlich, Martino Pesaresi, Thomas Kemper, Marcello Schiavina, Sergio Freire, and Michele Melchiorri

Abstract Societal inequalities manifest at a range of scales, from coarse (inter-continent) to fine (intra-city). Satellite-measured night-time lights (NTL) have shown value for capturing and estimating socioeconomic characteristics, including economic activity, well-being, and poverty. However, multi-scale mapping and visualization of inequalities, especially their relative gradations and spatial patterns, have remained a challenge. To narrow this gap, we developed an approach that combines globally available built-up surface, population density, and night-time light intensity data. The integration of these earth observation-derived variables through a spatial visualization frame reveals patterns of societal inequalities at different scales. Our findings suggest that: (1) Outlining and mapping settlements using night-time lights alone underrepresent settlements of low-income countries, as both rural and suburbia of larger cities of the Global South are scarcely lit at night. (2) Combining population and built-up density that spatially locate people on the surface of the Earth with NTL provides insights on deprivation related to the lack of electricity and the services that come with it. (3) Night-time lights and inequality maps are the results of many factors that need to be addressed at different scales. A body of scientific literature that we review has just started to describe the variety of night-time light sources and the spatial variation within and across countries. New, fine-resolution NTL, population, and built-up density that are now becoming available may provide additional insights.

Keywords Societal inequalities · Night-time lights · Spatial visualization · Population density

D. Ehrlich (✉) · M. Pesaresi · T. Kemper · M. Schiavina · S. Freire · M. Melchiorri
European Commission, Joint Research Centre, Ispra, Italy
e-mail: daniele.ehrlich@ec.europa.eu

M. Kuffer, S. Georganos (eds.), *Urban Inequalities from Space*, Remote Sensing and Digital Image Processing 26, https://doi.org/10.1007/978-3-031-49183-2_3

3.1 Introduction

In a world populated by eight billion people, quantifying the human presence and inequalities is essential to devise strategies to combat poverty and understand sustainability and the resilience of societies. Inequality is used to indicate issues including deprivations, particularly in health, education, safe water and sanitation, nutrition, and consumption (World Bank Group 2016), as well as in access to economic and infrastructure resources (Pandey et al. 2022; United Nations 2020). In this research, we refer to inequality as a lack of light at night in human settlements, presumably due to the inability to access electricity and the services that electricity can provide to households, communities, and societies.

Measuring inequalities among and within human societies has always been a challenge. Society's access to resources differs greatly across planet Earth. On the one extreme are the low-income subsistence farming communities in remote and predominantly rural landscapes, or those that live in the low-income peripheries of the metropolises of the Global South. On the other extreme are high-income communities and energy-producing countries – including those that can prosper also in otherwise inhospitable locations on Earth thanks to the ability to access all possible goods and services through their income. Such communities are typically located in high-income or energy-producing societies, where electricity is ubiquitous and available to illuminate all types of physical infrastructure.

The demand for global spatially consistent population data and their attributes including inequality is expressed indirectly through a large body of policy and scientific documents addressing poverty and the sustainability of planet Earth. For example, attaining the Sustainable Development Goals (SDGs) is based on a set of related indicators that need to be monitored and reported periodically (Anderson et al. 2017). Directly relevant to this work is SDG 1, which aims to "End poverty in all its forms everywhere"; SDG 7 to "Ensure access to affordable, reliable, sustainable and modern energy for all," which is one key socioeconomic indicator; and SDG 11 aims to "Make cities and human settlements inclusive, safe, resilient and sustainable."

Consistent and global data on built-up areas have been made available in recent years. Global Earth observation image collections have been used to generate global land cover and land use maps (Gong et al. 2013) that include impervious class, as well as built-up from optical imagery (Pesaresi et al. 2016a, b) and from radar imagery (Esch et al. 2017; Marconcini et al. 2020). Multi-temporal built-up mapping enabled assessing the process of global urbanization (Melchiorri et al. 2018), as well as to sizing and enumerating settlements.

A number of global population distribution products are now available that differ with respect to the population concept being mapped, the input data, and the physical variables to which the population is associated (Leyk et al. 2019). This work uses the concept of residential population density generated by combining earth observation–derived built-up information and population estimates from census data (Freire et al. 2016). The spatial allocation of people uses the built-up density as a single

covariate (Corbane et al. 2019). The built-up density and population density spatial grids are available at different spatial resolutions from the GHS 2019 public data release (Florczyk et al. 2019). The data suit applications span from the local/regional to global domains. Population density datasets can now be further combined to address inequalities, including the usage of night-time lights (NTL).

Open night-time satellite imagery with global coverage has been made available from the Operational Linescan System on board the Defense Mapping Satellite Program (OLS-DMSP) (Baugh et al. 2010; Román et al. 2018) and more recently by imagery originating from the visible infrared imaging radiometer suite (VIIRS) (Elvidge et al. 2017). Astronaut photographs of the Earth at night (available from http://eol.jsc.nasa.gov) have also been used to address city light emissions, although the limited number of cities covered makes it useful for local studies only. OLS-DMSP, VIIRS, and astronaut photographs have been used to address socio-economic characteristics including urban extent (Liu et al. 2019; Zhou et al. 2015), population density (Sutton et al. 2011), gross domestic product (GDP) (Galimberti 2020; Sutton et al. 2007; Wu et al. 2013), poverty (Elvidge et al. 2009), and development and other socioeconomic variables (Elvidge et al. 2012; Levin and Duke 2012; Nordhaus 2006).

A line of research equates the spatial distribution of night-time lights with access to electricity and the services that electricity supplies and links the lack of electricity with poverty or inequality. For example, geographical pockets of poverty are estimated by combining the "dark" regions as measured from VIIRS NTL with settlements (McCallum et al. 2022) defined by the World Settlement footprint (Marconcini et al. 2020). Similarly, poverty was spatially located by "dark" population spatial grids from LandScan (Dobson et al. 2000), as those areas that are not covered by NTL form the DMSP (Smith and Wills 2018). NTL has been considered for use in developing economic indicators (Chen and Nordhaus 2011) for countries with low-quality statistical data and economic growth (Henderson et al. 2012). Gridded built-up, population, and night-time lights combined have also been used in addressing regional-scale infrastructure development in India and in the United States to address progress towards the SDGs (Stokes and Seto 2019) and to map inequalities globally (Ehrlich et al. 2018).

Relevant to this work is the body of research that analyzed the sources of light recorded by the OLS-DMSP, VIIRS-NTL, and within-country and across-country variations. For example, Kyba et al. (2014), provided insights into the type of land uses that generate NTL. These authors also showed that in 2012, former East Germany cities emit more light per capita than those in former West Germany and that American cities emit more light per capita than the German cities. Levin and Duke (2012), identify and explain differences in emissions due to socioeconomic status of settlements in Israel and the Palestinian Authority. Nordhaus and Chen (2015), assessing GDP from NTL, reported that the lowest-income countries have also the lowest night-time recording and that these may be filtered out in the processing hampering the effort of gathering GDP statistics. Weidmann and Schutte (2017), report on the large discrepancy in NTL emissions from rich countries.

We propose a qualitative analysis of patterns of inequality based on a visualization of three global variables. We use built-up density and population density – two global variables that are co-produced to spatially locate settlements – and satellite-measured NTL. The three variables are also referred to as societal variables (Ehrlich et al. 2021) as they all are related to processes and patterns generated from human activities (Ehrlich et al. 2020).

We process the three variables with a unique set of parameters tailored to identify spatial patterns that have been reported in the literature or that we justify based on current knowledge. This research is thus a qualitative data exploration exercise that aims to assess the potential of the three variables combined to guide further research at global and regional scales. Finally, we discuss the limitations of the three variables taken separately, the limitations of the variables taken in combination, and the limitation of a single set of parameters, ending with an outlook on future possible research.

3.2 Data

This study uses three 1x1 km spatial grids generated for the nominal year 2015; the Global Human Settlement Built-up (GHS-BUILT), the Global Human Settlement Population (GHS-POP) (Florczyk et al. 2019), and the NTL from VIIRS NTL from the Black Marble Night Time Lights (Elvidge et al. 2017; Román et al. 2018).

3.2.1 GHS-Built

The GHS-BUILT layer quantifies the density of the built environment. More specifically, it provides a quantitative measure of the surface area covered by buildings (Corbane et al. 2019; Pesaresi et al. 2013). The GHS-BUILT is generated by processing a combination of image repositories, including that of Landsat-8-optical imagery multispectral bands for 2014 and 2015, available at 30 × 30 m and the Landsat panchromatic band available at 10 × 10 m. Symbolic machine learning (Pesaresi et al. 2016a, b) was used for information extraction, an association type of algorithm that allows to simultaneously process satellite information from different sources. The extracted built-up information is averaged – using a surface share function – over 250 × 250 m spatial grids for use in generating GHS-POP, and in 1 × 1 km spatial grids to be used for the visual analysis of inequality in this research. All output data are available in World Mollweide equal area projection (EPSG 54009).

3.2.2 GHS-Pop

The GHS-POP is a spatial grid of residential population abundance and density. It is generated by combining census data from the Gridded Population of the World (GPW) with the GHS-BUILT. GPW (Center for International Earth Science Information Network-CIESIN-Columbia University, 2017) collects and integrates several available census data and estimates population counts for different epochs, adjusted at the national level to the 2015 United Nations World Population Prospects (United Nations 2015). Such population counts are linearly disaggregated from census units to GHS-BUILT 250 × 250 m grid cells, informed by the locations and density of built-up areas (Freire et al. 2016). For this analysis, the population layer is made available as 1x1 km grid cells for the year 2015, in World Mollweide equal area projection (EPSG 54009).

3.2.3 Night-Time Light Emissions

The night-time light emissions are collected by the visible infrared imaging radiometer suite (VIIRS day/night band (DNB) (Elvidge et al. 2017) generated by the Earth Observation Group (EOG) at the National Oceanic and Atmospheric Administration (NOAA/National Geophysical Data Center (NGDC) (Elvidge et al. 2017). We used Version 1 of VIIRS day/night band VIIRS-NTL (Elvidge et al. 2017, 2021). VIIRS-NTLs are filtered from radiance generated by a number of natural phenomena, including moonlight and aurora (Román et al. 2018). VIIRS-NTL shows cloud-free average radiance emitted, expressed as nano-watt per steradian per square centimeter (nW cm^{-2} sr^{-1}). The outlier removal process filters out fires and other ephemeral lights. The data are available as 15 arc-second spatial grids mapped to the WGS84 geographic coordinates, covering the globe from 75° latitude North to 65° latitude South. We use the annual average image composite products (Elvidge et al. 2021) for the reference year 2015. The data were processed and resampled for this research to a 1 × 1 km grid in World Mollweide projection (EPSG 54009) aligned with GHS-BUILT and GHS-POP grids.

3.3 Data Processing

The GHS-POP, GHS-BUILT, and NTL at 1 × 1 km grids were further processed to allow their combined visualization and interpretation. This included standardization, sequencing, encoding, and visualization (Ehrlich et al. 2018).

The statistical parameters – average and standard deviations – for visualization of the three variables are used for global, regional, or local visualization. For global representation, we collected statistics from all grid cells containing population higher

than 50 people (Box 3.1, Eq. 3.1). For regional and local representation, we collected statistics from all populated grid cells.

The standardization procedure aimed at adjusting the value range of each variable to that of the other two variables in order to allow for a meaningful visualization in the RGB color space. First, we rescaled the GHS-POP and NTL based on a logarithmic base 10 function (Box 3.1, Eq. 3.2). Second, we centered the data distribution of each variable to the dynamic range required for the visualization. That rescaling and data range adjustment used two standard deviations to define the minimum and maximum (Box 3.1, Eqs. 3.3, 3.4, and 3.5).

Box 3.1: Equations Used in Preprocessing the Variables for Visualization

(3.1) $d \in \{x : x_{GHS\_POP} > 50\}$.

(3.2) x.

(3.3) $x'' = \frac{(x' - c_{\min})}{(c_{\max} - c_{\min})}$ the linear rescaling of (1), bounded in the [0..1] interval.

(3.4) $c_{\max} = \mu_{x'_d} + 2\sigma_{x'_d}$

(3.5) $c_{\min} = \mu_{x'_d} - 2\sigma_{x'_d}$, with $\mu_{x'_d}$ being the average of x' in the spatial domain d, and $\sigma_{x'_d}$ being the standard deviation of x' in the same spatial domain d.

The clustering allows associating the standardized GHS-POP, GHS-BUILT, and NTL data to the additive color-mixing model as represented in the color cube model (Fig. 3.1). The combination of values from the three thematic layers is associated with the colors of the data cube scaled from 0 to 255. Vertices 1, 3, and 5 show, respectively, the primary colors red, green, and blue, with blue only showing grid cells with night-time light values NTL, red grid cells with only population counts, and green grid cells with only built-up areas. Vertices 2, 4, and 5, show respectively, the secondary colors, magenta, yellow, and cyan, with magenta showing both population and NTL but no built-up, yellow only population and built-up and no night-time lights, and cyan only built-up and night-light and no population. The colors in between vertices indicate combinations of the three variables. Vertex 7 corresponds to white, with all variables showing the highest value. Vertex 8 corresponds to black, with all values corresponding to 0. The prevalence of one color over the other represents the relative dominance of one societal variable over the other variables.

3.4 Results

The combinations of the three societal variables in visual band composites generate spatial color patterns that can be related to different settlement pattern characteristics. Table 3.1 summarizes the association between colors as from the color cube of

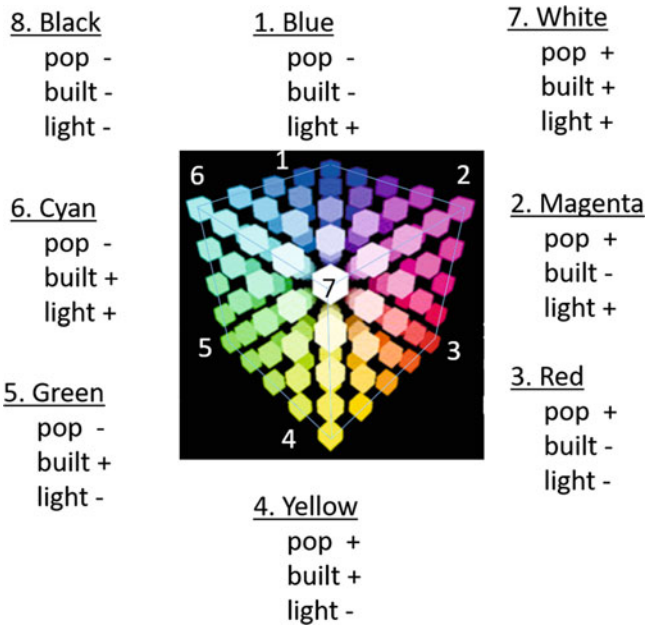

Fig. 3.1 Color cube showing all possible color combinations used to visualize societal inequality generated from population density, built-up density, and night-light emissions

Fig. 3.1 and the relative presence of the corresponding societal variables and the spatial settlement patterns that can be detected. The following sections provide examples of colored spatial patterns that focus on identifying spatial inequalities at global, regional, and local scales. We also compare local scale inequality patterns across continents and in disaster-affected areas. We selected the inequality maps presented in this research based on the societal patterns and processes that we could understand and explain. When considered relevant, we combine inequality maps with NTL maps representing the same geographical area. For cartographic rendering purposes, global maps are resampled to 5 × 5 km, while all other maps are generated using statistics from the 1 × 1 km spatial grids.

3.4.1 Global Inequality Maps

Global inequality maps show populated areas of the world with different color patterns (Fig. 3.2). All major cities are characterized by white colors given their concentration of population, built-up, and illumination, but not everywhere. Figure 3.2 shows in red tones the inhabited areas of the world poorly lit and present in Sub-Saharan Africa, parts of Asia, and Latin America. The blue tones – characterized by NTL that dominates over the built-up and population – occur in the

Table 3.1 Correspondence between colors as represented in the color cube of Fig. 3.1, relative values of societal variables, and example of settlement patterns

Color cube vertices	Colors	Societal variables relative values (abbreviations for figure legends)	Examples of settlement pattern characteristics
1	Blue	High NTL, less population, and built-up (P−B−L+)	Large industrial installations, security infrastructures, oil and gas extraction sites, illuminated road infrastructure
2	Magenta	Population, NTL, and less built-up (P + B−L+)	Deprived areas, dense urban centers, densely inhabited
3	Green	Built-up, less NTL, and less population (P−B + L−)	Overbuilt rural areas, abandoned villages, overbuilt rural areas
4	Yellow	Population, built-up, and less NTL (P + B + L−)	Poor-lit cities, deprived areas, historic urban centers, diffuse settlements, scarce public illumination. Disaster-affected urban areas
5	Red	Mostly population, less built-up, and NTL (P + B−L−)	Deprived areas, dense population, and absence of public illumination. War-affected areas, disaster-affected rural areas, urban areas in low-income neighborhoods
6	Cyan	Built-up, NTL, and no population (P−B + L+)	Affluent cities, suburbs, large built-up land use, large public illumination, sparse population
7	White	Population, built-up, and NTL (P + B + L+)	Well-lit cities resulting from high density of people, high density of buildings, large night-light emissions
8	Black	No population, built-up, and NTL (P−B−L−)	Locations on earth with no human presence

high-income or energy-producing countries. The most visible blue tone occurs in North America, in the larger cities of South America, parts of Europe, oil-producing countries of the Middle East, South Korea, and Taiwan, which are also middle- or high-income countries. The green color indicates higher values of built-up relative to population and night-lights and that occurs in high and medium-income countries. Yellow spatial patterns showing a very high concentration of population and built-up are found around the megacities of the eastern part of the Indian subcontinent and the Eastern lowlands of China.

3.4.2 Regional Inequality Maps

Regional inequality maps provide insight on differences between countries or countries belonging to similar income class. Figure 3.3 shows North America and part of the Caribbean region. A large part of the United States is shown in blue, the typical color combination of high-income countries. All larger cities show most of

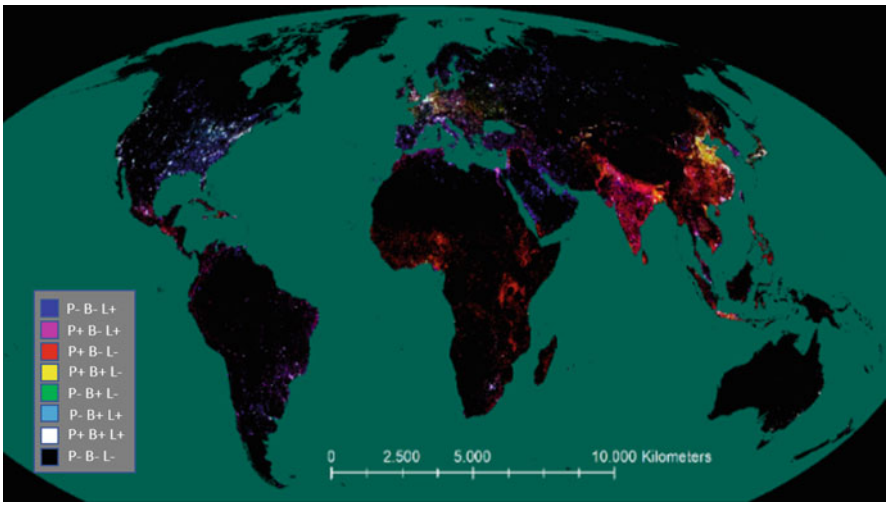

Fig. 3.2 Global spatial pattern of inequality map represented as combination of colors using data aggregated at pixel of 5 × 5 km large grid cells. The color legend indicates population (P), built-up (B), and night-time lights (L) with relative abundance (+) or scarcity (−). Colors indicate spatial societal patterns with high-income regions in blue, low-income regions in red, and colored in between including high populated with high density of built-up – yellow tones in east Asia – and high population with lower density of built-up in cyan

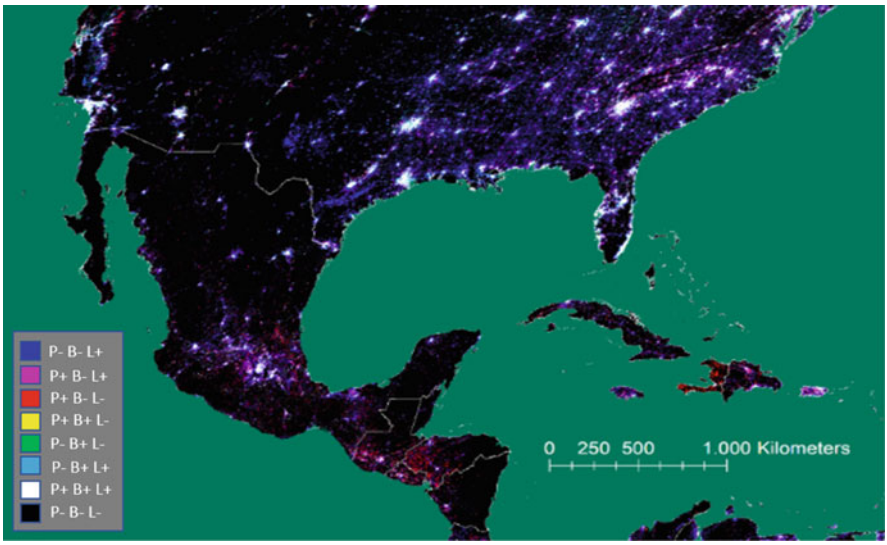

Fig. 3.3 Inequality map for North America and part of the Caribbean. The United States shows well-lit patterns in large cities and smaller settlements. Mexico and the Caribbean show well-lit cities and less well-lit rural areas. The color legend indicates population (P), built-up (B), and night-time lights (L) with relative abundance (+) or scarcity (−)

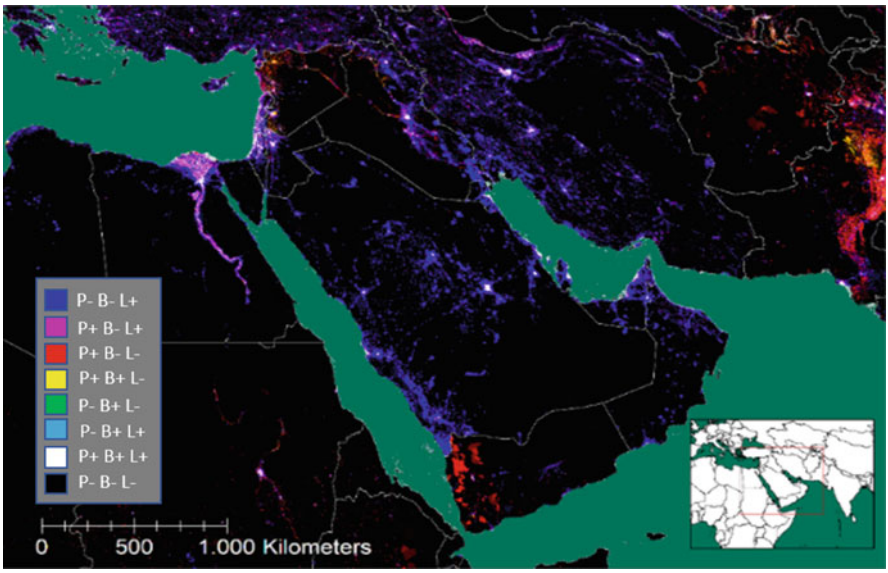

Fig. 3.4 Inequality map for Middle East. The color legend indicates population (P), built-up (B), and night-time lights (L) with relative abundance (+) or scarcity (−).The map shows the high-income and oil-producing countries in blue, the emerging economies in cyan (i.e., Egypt, Nile Delta), countries in conflict (i.e., Yemen, Syria, and Northern Iraq), and low-income countries (i.e., Afghanistan) in red

their area covered in white, indicating a relatively high value for population, built-up, and NTL. The more densely populated settlements of the East of North America indicate less built-up, which may be related to the higher concentration of larger buildings. The figure also shows dark blue related to the oil field of Texas (Southern United States). The color spatial pattern differs for Mexico and the Caribbean region. Mexico city and the larger cities show high built-up, population, and night-lights as in high-income country. The remaining settlements colored in red indicate low built-up and NTL.

Figure 3.4, a regional map of the Middle East, is centered on the Arabic peninsula and shows a number of spatial inequality patterns. Saudi Arabia and part of Iraq are characterized by blue color with a high degree of NTL. In the southernmost part of the peninsula, coinciding with Yemen, the tones are red, indicating a lack of night-light and relatively low built-up densities. This part coincides with conflict areas where lights are off (Jiang et al. 2017). The Nile Delta (Egypt) is characterized by high population and NTL, and this is in contrast with the southern part of the Nile River in Sudan, where NTLs are completely absent with the exception of Sudan's capital Khartoum. The figure also shows the moderately well-lit part of Turkey and the lack of night-lights in Syria and part of Northern Iraq due to the ongoing conflict that unfolded in 2015.

Europe's inequality spatial patterns are particularly diverse across the continent and originate from a number of societal processes (Fig. 3.5). These inequality

Fig. 3.5 Inequalities in Europe and Europe's neighborhoods. The color legend indicates population (P), built-up (B), and night-time lights (L) with relative abundance (+) or scarcity (−)

patterns are determined by a combination of the settlement sizes and spatial distribution, as well as that of NTL emissions. For example, in the Po River valley (Italy), settlements are relatively small and dispersed, while those found in Southern Italy are more concentrated despite similar night-light emissions. We describe below the more significant continental patterns as a systematic review of the origin and source of all NTL is beyond the scope of this work. Figure 3.5 shows mountain regions, including the Alps, Carpathian Mountains, as well as the Apennines as largely not lit and unpopulated. All larger cities are well lit. Areas in between large cities differ as Southern Europe is more lit than central and eastern Europe.

Figure 3.6 illustrates patterns of inequality in East Asia, including Western China, Korea, and Japan. Most noticeable is North Korea and South Korea night-time light divide. North Korea is not well lit except for the capital. South Korea is well lit similar to other high-income countries. Japan shows high night-time use in cities but low NTL in the peripheries. This, combined with a high land per capita ratio in a rural area, makes it a unique societal pattern. Very noticeable also is China with very well-lit cities, while the rural area – densely populated with a large number of small towns closely spaced – is not well lit, generating a unique spatial pattern characterized by a high density of population and built-up displayed in yellow.

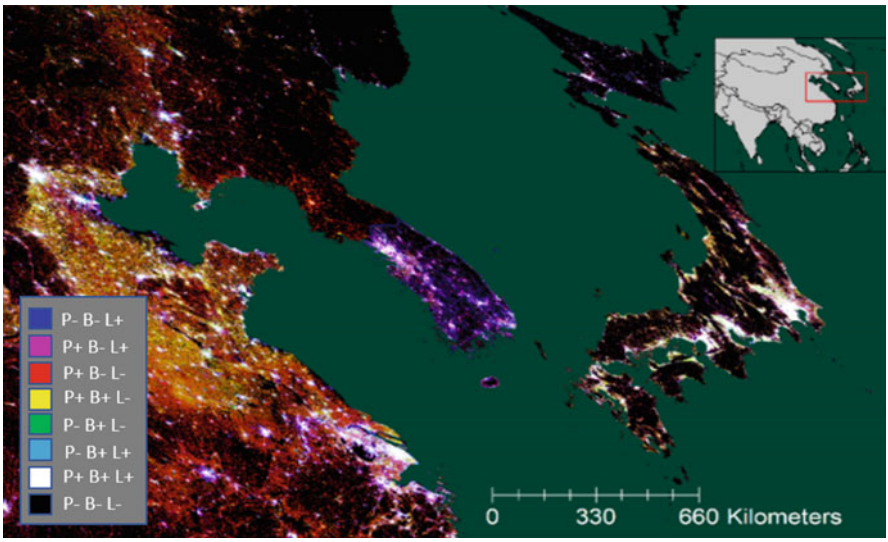

Fig. 3.6 South and North Korea show different night-time spatial patterns. South Korea is well illuminated, while North Korea is very poorly lit. The color legend indicates population (P), built-up (B), and night-time lights (L) with relative abundance (+) or scarcity (−)

3.4.3 Across Continent Inequality

Figure 3.7 shows inequality maps for four 80x240 km large areas in four continents (a1–d1) and the corresponding NTL maps (a2–d2). Figure 3.7 – a1 shows part of the Po River plain (Italy), including Torino as the largest settlement, and Fig. 3.7 – a2 shows the corresponding NTL map. Figure 3.7 – a1 and a2 show a nearly complete coverage of night-lights for both larger cities and smaller settlements scattered within the agricultural land. As from the legend, the larger cities and towns with high population, built-up, and NTL appear in white. The cyan color indicates a relatively high value of NTL and built-up with lower density of population characteristics of productive infrastructure – commercial and industry – as from Fig. 3.1.

Figure 3.7 – b1 and b2 show the agricultural region in the central plains of the United States extending between Iowa City and Davenport. The region shows mostly towns and cities, and all larger towns are lit at night (Fig. 3.7 – b2). The combination of spatial settlement patterns and illumination highlights the areas populated as well as the more commercial and productive areas represented in cyan.

Figure 3.7 – c1 and c2 are centered on the city of Shijiazhuang in Hebei province, which covers the rich agricultural land of Eastern China plains. Only the large- and medium-size cities are lit at night, as shown in Fig. 3.7 – c2. The rural areas are interspersed by a dense pattern of towns spatially located at regular distances from

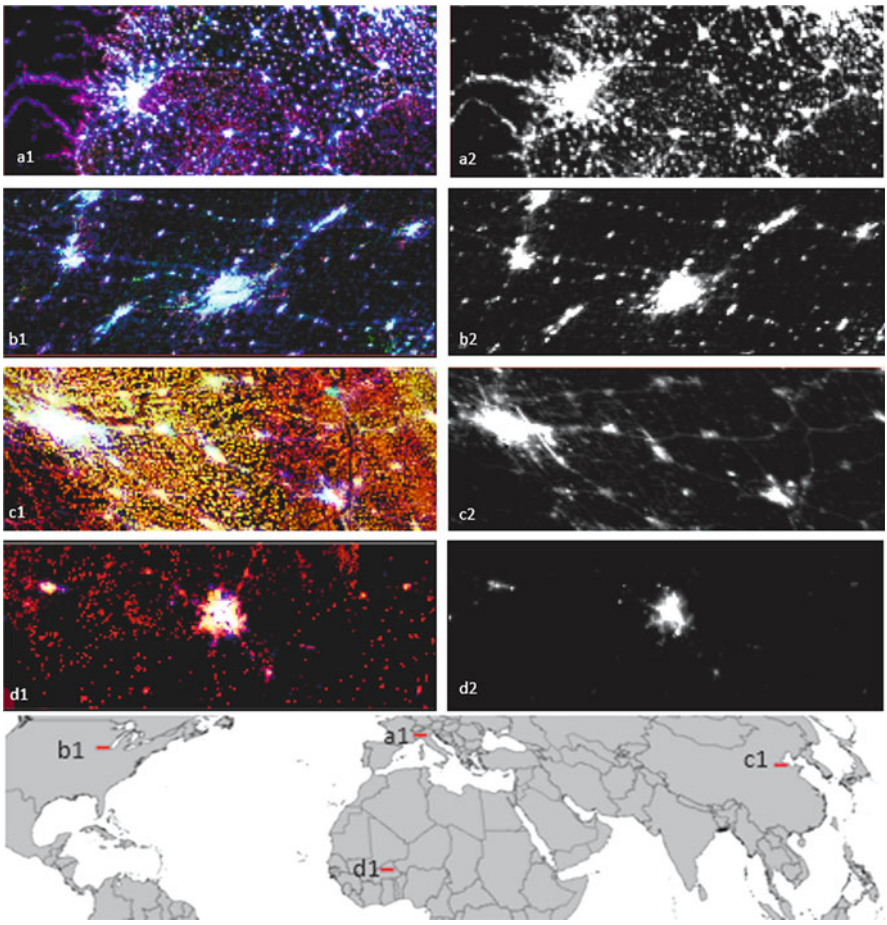

Fig. 3.7 Inequality maps (a1, b1, c1, d1) and NTL maps (a2, b2, c2, d2) for four 80 × 240 km regions centered on: (**a**) Torino (Italy), (**b**) Davenport (USA), (**c**) Shijiazhuang (China), and (**d**) Ouagadougou (Burkina Faso)

each other. At the 1 × 1 km spatial resolution, this pattern of settlements is rendered as a continuous built environment. The area is densely inhabited, and this generates typical yellow patterns from the dominance of built-up and population with lower NTL.

Figure 3.7 – d1 and d2 show rural areas centered in Sub-Saharan Africa along the Sahel belt, with Ouagadougou (Mali) as the largest settlement. The region outside Ouagadougou is inhabited, but not lit at night. Red is the typical color for highly populated areas with low density of built-up and no light.

3.4.4 *Local and Disaster-Related Inequality Maps*

Figure 3.8 shows a divide between Haiti, the Dominican Republic, and Puerto Rico. Puerto Rico exhibits high-income style of high illumination throughout the island. The Dominical Republic shows well-lit urban areas and towns interspersed with poorly illuminated rural areas. In strong contrast is Haiti, where only the capital Port Au-Prince is illuminated and with lower intensity than other capitals.

Local night-time lights and inequality maps show finer-scale inequality patterns. Figure 3.9 compares NTL (Fig. 3.9 – left) and inequality (Fig. 3.9 – right) for parts of Southern Nigeria. At this cartographic representation, the night-time map shows

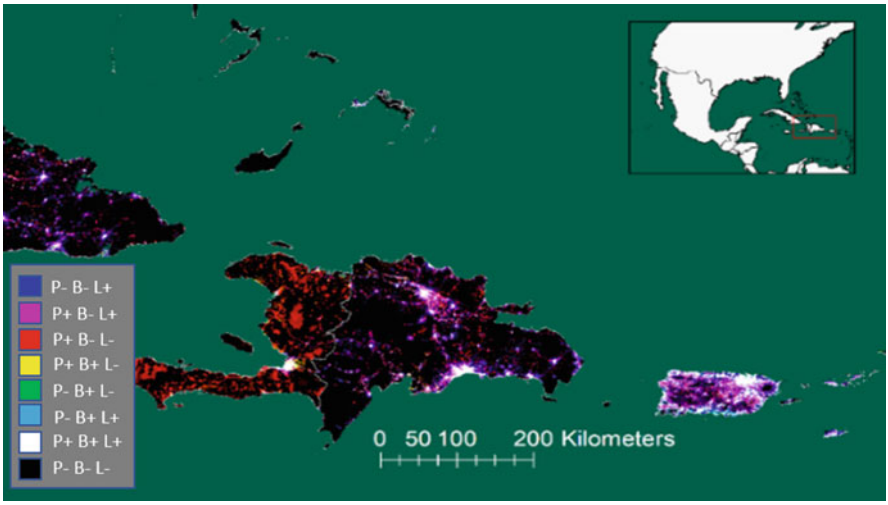

Fig. 3.8 Inequality map depicting Haiti, Dominican Republic, and Puerto Rico. The color legend indicates population (P), built-up (B), and night-time lights (L) with relative abundance (+) or scarcity (−)

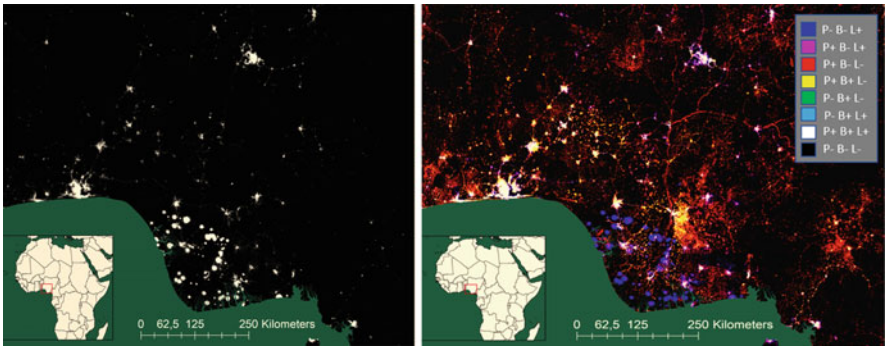

Fig. 3.9 Nigh-time lights, map (left) and inequality map for Southern Nigeria (right)

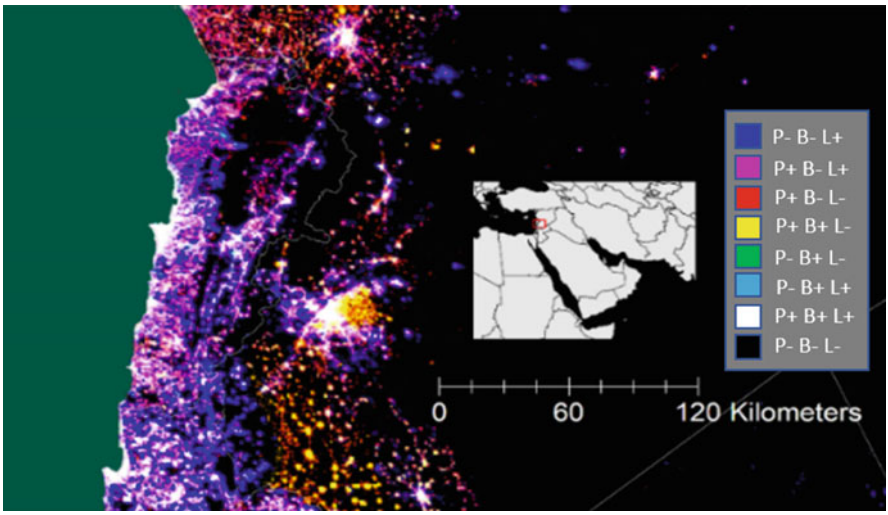

Fig. 3.10 Conflict related inequality map for 2015 centered on Syria. The color legend indicates population (P), built-up (B), and night-time lights (L) with relative abundance (+) or scarcity (−)

major cities including Lagos and Abuja and some secondary cities well lit. The oil extraction sites in the Niger delta are also well lit due to gas flares and presumably for security reasons. However, the inequality maps show the blue tones indicating the absence of population and built-up. The NTL figure also shows some secondary cities and some scattered settlements in between cities. The inequality map includes many more settlements (color coded in red) that are not lit, as shown from the NTL map. Larger and smaller cities show diminishing availability of electricity moving from the center to the peripheries and displayed in yellow. Only Abuja shows peripheries with high built-up and light and low population shown in magenta.

NTLs are used to report on disaster-affected areas. In fact, electricity supply is often disrupted by the impact of hazards (Cole et al. 2017) and is best observable with NTL taken days or weeks apart. Protracted crises can be detected also from night-time annual averages. Figure 3.10 shows the outcome of the protracted conflict in Syria, still unfolding in 2015. Figure 3.10 also shows Damascus with one part of the city – the government controlled – well lit, and the eastern part of the city from the opposing forces not lit (yellow shades). Most of the rural areas south of the capital are not lit except for the larger city (European Commission, Joint Research Centre 2016).

3.5 Discussion

The chapter describes a procedure to visualize inequality patterns using three earth observation–derived products processed with a unique set of parameters. This visual data exploration approach confirms the usefulness of combining NTL, population,

and built-up to detect inequality linked to income, access to resources, and disaster-related electricity supply disruptions. We show that inequality patterns are visible at global, regional, and local scales, and each scale of representation has benefits and limitations in visualizing societal patterns and processes. For the global representation, we have aggregated the 1 × 1 km grids to the coarser 5 × 5 km spatial grids. The global overview displays the economic areas of the globe with the high-income countries and the oil-producing countries – with high NTL densities, the middle-income countries with a high variety of NTL densities, and the low-income countries with NTL mostly detected only for major urban areas. The drawback of global representations is the inability to show very sparse settlement patterns in part due to cartographic representation limitations. In fact, the color rendering at coarse scales are modulated by the amount of information that can be displayed. The benefit of this global representation consists in the spatial consistency of representation across the globe.

The continental and country level representation at 1 × 1 km grid resolution reflects the countries' diverse income and policies related to night-time emissions. For example, Fig. 3.4 centered on the Middle East shows that the high-income and energy-producing countries are in stark contrast with the lower-income countries. In Europe, the spatial inequality patterns vary considerably despite the countries having similar access to energy and income. There are considerable differences even within a single country, i.e., former West and East Germany. Also, east European countries lit cities and urban areas better than rural areas; while southern European Countries and North African countries show high NTL emissions for all settlements.

Africa displays two main patterns, that of Northern and Southern Africa with NTL both in urban centers and in rural areas, and that of sub-Saharan Africa with low coverage of NTL except for the larger cities. Asia shows great variability related to the different population concentrations and night-time emissions.

Middle-income country spatial patterns are diverse and are in part due to the different use of night-time illumination, including different urbanization textures and population density. At the country scale, inequality can be often detected across borders of countries with different incomes and/or within a single country due to conflict of natural hazard impact.

In this research, the city-wide inequalities are shown for selected Syrian cities. We confirm our findings reported in the literature that disaster-affected areas typically have disruptions in energy supply and that disruptions can be detected for disaster-affected regions. In fact, we expect to detect NTL shortcomings also in deprived and in informal settlements or slums. However, within-city NTL emission variations should be measured with sensors of higher resolution than that of VIIRS.

The 1 × 1 km spatial grids of population built-up density and NTL used in this research are not optimal for locating deprived areas or not lit areas within cities. Built-up is generally detected in deprived areas at the original spatial resolution from which built-up is extracted. The aggregation of the built-up and the derived population information into 1 × 1 km grid inevitably decreases the precision that is required to outline those city sections. In addition, deprived areas are often nested within more affluent parts of the city and the "glowing" effect of NTL emissions

over the more affluent areas may extend over non-lit areas especially when using weekly, monthly, or annual average products. Finally, the cities of the Global South, those that often host slums, are already poorly lit, making it even more difficult to locate deprived areas. The usefulness of night-light analysis for deprived areas would be best addressed using higher-resolution imagery as that from the new generation of night-time sensors and/or from astronaut photography.

The reader should always be knowledgeable about the limitations of the three input data used in this research. GHS-BUILT data are generated from artificial intelligence procedures and that process is not error free. Typically, errors are more likely to occur in regions of sparse settlements and less in dense urban areas. From our analysis, informal settlements and deprived areas within larger cities are detected from the processing of Landsat imagery. Future research will quantify the accuracies across settlement patterns and the impact of these patterns on color rendering.

GHS-POP relies on census data that are not always up to date for all countries of the world. Moreover, the population distribution accuracy is likely to be different across space, and it depends on the spatial and geometrical accuracy of the census data. With coarse census units as those available in many low-income countries, the census number is disaggregated to any built-up feature detected including that of the deprived areas. Finally, GHS-POP that used a resident population relies on improving the spatial distribution for residential and non-residential areas, as well as to include the volume of built-up that is the ultimate measure for attempting to measure floor space per person.

NTL for use in assessing societal activities also need to be assessed. First, the satellite overpass at 1.30 am images is not ideal to represent societal activity that would be more representative, if the satellite would fly over before midnight. Also, the sensor may not be able to detect faint lights simply due to the imaging resolution and the sensibility of the sensor (Elvidge et al. 2021). The annual averages represent stable lights over the year. This averages out images that may be illuminated for a short period of time. In fact, while all the oil-producing sites are being detected, wild forest fires are not detected. This analysis also shows that protracted crises that suffer prolonged electricity shut downs can be detected, those occurring at short intervals and that are quickly restored cannot be detected from annual averages.

3.6 Conclusions

The chapter describes a procedure to visualize societal inequalities related to the access to electricity and the services it provides, the availability of built infrastructure, and the resident population. The topic is of relevance for addressing disparities in access to resources and services associated to electricity and to locate low-income communities; all topics are relevant to the post-2015 Development Agenda. We could infer societal regional patterns that are consistently occurring in different parts of the world and reported in the literature. We would also like to report that as NTLs

are not detectable for part of the world, these may provide biased results if used to outline human settlements. In fact, large parts of rural landscapes in Sub-Saharan Africa and Asia do not appear to be lit at night but are often densely populated. Also, while most large cities of the globe are all well lit, a number of large cities of the Global South are only partly lit. Many cities show to be lit at the city center and night-light rapidly decrease from the center to the peripheries. The high-income countries typically are all very well lit. Some, high-income oil-producing countries show NTLs for all settlements as well as for the transport infrastructure connecting settlements.

There is regional difference within continents. There are inequalities to be noted between North America and Latin America, as well as for many countries in East Asia. There are some strong gradients along the border of neighboring countries with striking examples in the border separating North and South Korea as well as Haiti and Dominican Republic. There are also inequalities within the same country that can be observable due to prolonged effect of hazard impact or conflict. Urban inequalities are unlikely to be detected from the variables at the 1 × 1 km resolution. Finer resolution NTL and finer spatial resolution built-up grids should be used instead.

This first attempt that explores night-lights and the combination with built-up and population densities shows a promising avenue of research especially for global, continental, and country-wide inequality description. In fact, NTL should also be considered an essential societal variable (Ehrlich et al., 2021) used in addressing societal patterns and processes (Ehrlich et al. 2020). This research opens new ways of investigation especially when new finer resolution night-time light will be available. First, we will continue to explore the new NTLs that are generated by new sensors, including that onboard the SDGSAT-1 (Hu et al. 2022). Second, we will use the new night-time series for 2020 and include in the analysis the new GHS-BUILT dataset generated with Sentinel-2 data that is mapping building densities much more refined. This will have an effect on the population distribution in particular in developing countries, where the new data may show even more people in rural areas deprived of access to electricity. Combining the three variables at finer resolution may reveal new spatial patterns originating from processes that are averaged out from the current coarse datasets. Third, we will attempt a more systematic data standardization procedure for a systematic assessment of inequality maps over time. Fourth, we will assess relations with inequality indicators derived from these datasets with data collected in the field. Future research will also address the use of night-time lights to understand and monitor the impact of night-time light in the natural environment as light pollution is an issue for the natural world, as well as to monitor use and/or efficiency in the use of resources.

References

Anderson K, Ryan B, Sonntag W, Kavvada A, Friedl L (2017) Earth observation in service of the 2030 agenda for sustainable development. Geo-spatial Inf Sci 20:77–96. https://doi.org/10.1080/10095020.2017.1333230

Baugh K, Elvidge CD, Ghosh T, Ziskin D (2010) Development of a 2009 stable lights product using DMSP-OLS data. APAN Proc 30:114. https://doi.org/10.7125/APAN.30.17

Center for International Earth Science Information Network-CIESIN-Columbia University (2017) Gridded population of the world, version 4 (GPWv4): population count, revision 10. https://doi.org/10.7927/H4PG1PPM

Chen X, Nordhaus WD (2011) Using luminosity data as a proxy for economic statistics. Proc Natl Acad Sci 108:8589–8594. https://doi.org/10.1073/pnas.1017031108

Cole T, Wanik D, Molthan A, Román M, Griffin R (2017) Synergistic use of nighttime satellite data, electric utility infrastructure, and ambient population to improve power outage detections in urban areas. Remote Sens 9:286. https://doi.org/10.3390/rs9030286

Corbane C, Pesaresi M, Kemper T, Politis P, Florczyk AJ, Syrris V, Melchiorri M, Sabo F, Soille P (2019) Automated global delineation of human settlements from 40 years of Landsat satellite data archives. Big Earth Data 3:140–169. https://doi.org/10.1080/20964471.2019.1625528

Dobson J, Bright E, Coleman P, Durfee R, Worley B (2000) A global population database for estimating population at risk. Photogramm Eng Remote Sens 66:849–857

Ehrlich D, Schiavina M, Pesaresi M, Kemper T (2018) Detecting spatial patterns of inequalities from remote sensing – towards mapping of deprived communities and poverty (No. EUR 29465). European Commission, Luxembourg: Publications Office of the European Union

Ehrlich D, Balk D, Sliuzas R (2020) Measuring and understanding global human settlements patterns and processes: innovation, progress and application. Int J Digit Earth 13:2–8. https://doi.org/10.1080/17538947.2019.1630072

Ehrlich D, Freire S, Melchiorri M, Kemper T (2021) Open and consistent geospatial data on population density, built-up and settlements to analyse human presence, societal impact and sustainability: a review of GHSL applications. Sustainability 13:7851. https://doi.org/10.3390/su13147851

Elvidge CD, Sutton PC, Ghosh T, Tuttle BT, Baugh KE, Bhaduri B, Bright E (2009) A global poverty map derived from satellite data. Comput Geosci 35:1652–1660. https://doi.org/10.1016/j.cageo.2009.01.009

Elvidge CD, Baugh KE, Anderson SJ, Sutton PC, Ghosh T (2012) The night light development index (NLDI): a spatially explicit measure of human development from satellite data. Soc Geogr 7:23–35. https://doi.org/10.5194/sg-7-23-2012

Elvidge CD, Baugh K, Zhizhin M, Hsu FC, Ghosh T (2017) VIIRS night-time lights. Int J Remote Sens 38:5860–5879. https://doi.org/10.1080/01431161.2017.1342050

Elvidge CD, Zhizhin M, Ghosh T, Hsu F-C, Taneja J (2021) Annual time series of global VIIRS nighttime lights derived from monthly averages: 2012 to 2019. Remote Sens 13:922. https://doi.org/10.3390/rs13050922

Esch T, Heldens W, Hirner A, Keil M, Marconcini M, Roth A, Zeidler J, Dech S, Strano E (2017) Breaking new ground in mapping human settlements from space – the global urban footprint. ISPRS J Photogramm Remote Sens 134:30–42. https://doi.org/10.1016/j.isprsjprs.2017.10.012

European Commission. Joint Research Centre (2016) Monitoring the Syrian humanitarian crisis with the JRC's global human settlement layer and night-time satellite. Publications Office, LU

Florczyk AJ, Corbane C, Ehrlich D, Freire S, Kemper T, Maffenini L, Melchiorri M, Pesaresi M, Politis P, Schiavina M, Sabo F, Zanchetta L, European Commission, Joint Research Centre (2019) GHSL data package 2019: public release GHS P2019

Freire S, MacManus K, Pesaresi M, Doxsey-Whitfield E, Mills J (2016) Development of new open and free multi-temporal global population grids at 250 m resolution. In: Proceedings of AGILE 2016. Presented at the AGILE 2016, Helsinki

Galimberti JK (2020) Forecasting GDP growth from outer space. Oxf Bull Econ Stat 82:697–722. https://doi.org/10.1111/obes.12361

Gong P, Wang J, Yu L, Zhao Y, Zhao Y, Liang L, Niu Z, Huang X, Fu H, Liu S, Li C, Li X, Fu W, Liu C, Xu Y, Wang X, Cheng Q, Hu L, Yao W, Zhang H, Zhu P, Zhao Z, Zhang H, Zheng Y, Ji L, Zhang Y, Chen H, Yan A, Guo J, Yu L, Wang L, Liu X, Shi T, Zhu M, Chen Y, Yang G, Tang P, Xu B, Giri C, Clinton N, Zhu Z, Chen J, Chen J (2013) Finer resolution observation and monitoring of global land cover: first mapping results with Landsat TM and ETM+ data. Int J Remote Sens 34:2607–2654. https://doi.org/10.1080/01431161.2012.748992

Henderson JV, Storeygard A, Weil DN (2012) Measuring economic growth from outer space. Am Econ Rev 102:994–1028. https://doi.org/10.1257/aer.102.2.994

Hu Z, Zhu M, Wang Q, Su X, Chen F (2022) SDGSAT-1 TIS prelaunch radiometric calibration and performance. Remote Sens 14:4543. https://doi.org/10.3390/rs14184543

Jiang W, He G, Long T, Liu H (2017) Ongoing conflict makes Yemen dark: from the perspective of nighttime light. Remote Sens 9:798. https://doi.org/10.3390/rs9080798

Kyba C, Garz S, Kuechly H, de Miguel A, Zamorano J, Fischer J, Hölker F (2014) High-resolution imagery of earth at night: new sources, opportunities and challenges. Remote Sens 7:1–23. https://doi.org/10.3390/rs70100001

Levin N, Duke Y (2012) High spatial resolution night-time light images for demographic and socio-economic studies. Remote Sens Environ 119:1–10. https://doi.org/10.1016/j.rse.2011.12.005

Leyk S, Gaughan AE, Adamo SB, de Sherbinin A, Balk D, Freire S, Rose A, Stevens FR, Blankespoor B, Frye C, Comenetz J, Sorichetta A, MacManus K, Pistolesi L, Levy M, Tatem AJ, Pesaresi M (2019) The spatial allocation of population: a review of large-scale gridded population data products and their fitness for use. Earth Syst Sci Data 11:1385–1409. https://doi.org/10.5194/essd-11-1385-2019

Liu X, de Sherbinin A, Zhan Y (2019) Mapping urban extent at large spatial scales using machine learning methods with VIIRS nighttime light and MODIS daytime NDVI data. Remote Sens 11:1247. https://doi.org/10.3390/rs11101247

Marconcini M, Metz-Marconcini A, Üreyen S, Palacios-Lopez D, Hanke W, Bachofer F, Zeidler J, Esch T, Gorelick N, Kakarla A, Paganini M, Strano E (2020) Outlining where humans live, the world settlement footprint 2015. Sci Data 7:242. https://doi.org/10.1038/s41597-020-00580-5

McCallum I, Kyba CCM, Bayas JCL, Moltchanova E, Cooper M, Cuaresma JC, Pachauri S, See L, Danylo O, Moorthy I, Lesiv M, Baugh K, Elvidge CD, Hofer M, Fritz S (2022) Estimating global economic well-being with unlit settlements. Nat Commun 13:2459. https://doi.org/10.1038/s41467-022-30099-9

Melchiorri M, Florczyk A, Freire S, Schiavina M, Pesaresi M, Kemper T (2018) Unveiling 25 years of planetary urbanization with remote sensing: perspectives from the global human settlement layer. Remote Sens 10:768. https://doi.org/10.3390/rs10050768

Nordhaus WD (2006) Geography and macroeconomics: new data and new findings. Proc Natl Acad Sci 103:3510–3517. https://doi.org/10.1073/pnas.0509842103

Nordhaus W, Chen X (2015) A sharper image? Estimates of the precision of nighttime lights as a proxy for economic statistics. J Econ Geogr 15:217–246. https://doi.org/10.1093/jeg/lbu010

Pandey B, Brelsford C, Seto KC (2022) Infrastructure inequality is a characteristic of urbanization. Proc Natl Acad Sci U S A 119:e2119890119. https://doi.org/10.1073/pnas.2119890119

Pesaresi M, Huadong G, Blaes X, Ehrlich D, Ferri S, Gueguen L, Halkia M, Kauffmann M, Kemper T, Linlin L, Marin-Herrera MA, Ouzounis GK, Scavazzon M, Soille P, Syrris V, Zanchetta L (2013) A global human settlement layer from optical HR/VHR RS data: concept and first results. IEEE J Sel Top Appl Earth Observ Remote Sens 6:2102–2131. https://doi.org/10.1109/JSTARS.2013.2271445

Pesaresi M, Ehrlich D, Ferri S, Florczyk AJ, Freire S, Halkia M, Julea A, Kemper T, Soille P, Syrris V (2016a) Operating procedures for the production of the global human settlement layer from landsat data of the epochs 1975, 1990, 2000, and 2014. Joint Research Centre, Luxembourg: Publications Office of the European Union

Pesaresi M, Syrris V, Julea A (2016b) A new method for earth observation data analytics based on symbolic machine learning. Remote Sens 8:399. https://doi.org/10.3390/rs8050399

Román MO, Wang Z, Sun Q, Kalb V, Miller SD, Molthan A, Schultz L, Bell J, Stokes EC, Pandey B, Seto KC, Hall D, Oda T, Wolfe RE, Lin G, Golpayegani N, Devadiga S, Davidson C, Sarkar S, Praderas C, Schmaltz J, Boller R, Stevens J, Ramos González OM, Padilla E, Alonso J, Detrés Y, Armstrong R, Miranda I, Conte Y, Marrero N, MacManus K, Esch T, Masuoka EJ (2018) NASA's black marble nighttime lights product suite. Remote Sens Environ 210:113–143. https://doi.org/10.1016/j.rse.2018.03.017

Smith B, Wills S (2018) Left in the dark? Oil and rural poverty. J Assoc Environ Resour Econ 5: 865–904. https://doi.org/10.1086/698512

Stokes EC, Seto KC (2019) Characterizing urban infrastructural transitions for the sustainable development goals using multi-temporal land, population, and nighttime light data. Remote Sens Environ 234:111430. https://doi.org/10.1016/j.rse.2019.111430

Sutton PC, Elvidge CD, Ghosh T (2007) Estimation of gross domestic product at sub-national scales using nighttime satellite imagery. Int J Ecol Econ Stat 8:5–21

Sutton PC, Elvidge CD, Baugh K, Ziskin D (2011) Mapping the constructed surface area density for China. Proc Asia-Pacific Adv Netw 31:69. https://doi.org/10.7125/APAN.31.8

United Nations (2015) World population prospects: the 2015 revision, key findings and advance tables

United Nations (ed) (2020) Inequality in a rapidly changing world, world social report. United Nations, New York

Weidmann NB, Schutte S (2017) Using night light emissions for the prediction of local wealth. J Peace Res 54:125–140. https://doi.org/10.1177/0022343316630359

World Bank Group (2016) Poverty and shared prosperity 2016: taking on inequality. World Bank, Washington, DC. https://doi.org/10.1596/978-1-4648-0958-3

Wu J, Wang Z, Li W, Peng J (2013) Exploring factors affecting the relationship between light consumption and GDP based on DMSP/OLS nighttime satellite imagery. Remote Sens Environ 134:111–119. https://doi.org/10.1016/j.rse.2013.03.001

Zhou Y, Smith SJ, Zhao K, Imhoff M, Thomson A, Bond-Lamberty B, Asrar GR, Zhang X, He C, Elvidge CD (2015) A global map of urban extent from nightlights. Environ Res Lett 10:054011. https://doi.org/10.1088/1748-9326/10/5/054011